
000 001 002 003 004 005 006 007 008 009 010 011 012 013 014 015 016 017 018 019 020 021 022 023 024 025 026 027 028 029 030 031 032 033 034 035 036 037 038 039 040 041 042 043 044 045 046 047 048 049 050 051 052 053 SYNCHRONIZING PROBABILITIES IN MODEL-DRIVEN LOSSLESS COMPRESSION

005 **Anonymous authors**

006 Paper under double-blind review

ABSTRACT

011 It is well-known in the field of lossless data compression that probabilistic next-
012 symbol prediction can be used to compress sequences of symbols. Deep neural
013 networks are able to capture rich dependencies in data, offering a powerful means
014 of estimating these probabilities and hence an avenue towards more effective com-
015 pression algorithms. However, both compressor and decompressor must have ex-
016 actly matching predictions; even small non-deterministic differences (which often
017 happen with learned models due to hardware, software, or computation order)
018 can lead to cascading decoding failures. In this paper, we formalize the problem
019 of prediction mismatch in model-driven compression, and introduce Probability
020 Matching Interval Coding (PMATIC), a model-agnostic algorithm that tolerates
021 bounded prediction mismatch with low overhead. PMATIC works with the pre-
022 dicted probabilities, making it compatible as a drop-in replacement for the arith-
023 metic encoder in model-driven compression tools. We show theoretical correct-
024 ness and performance bounds for PMATIC, and validate these results on text data.
025 These results confirm that, when paired an advanced prediction model, PMATIC is
026 robust to prediction mismatch while achieving compression rates that out-perform
027 standard modern compression tools.

1 INTRODUCTION

1.1 MODEL-DRIVEN LOSSLESS COMPRESSION

033 A key task in modern information systems is data compression, the process of reducing the size of
034 text, images, video, or other data so it can be stored and transmitted more efficiently. In lossless
035 compression, the data is encoded into a compact representation from which the original can be
036 decoded exactly, in contrast to lossy compression, which only permits approximate reconstruction.
037 Compression is generally formalized as the problem of encoding a string of discrete symbols drawn
038 from a finite alphabet. In deep learning contexts, these symbols are often referred to as tokens. The
039 choice of symbols is domain-dependent: for text, tokens are typically subword units or characters;
040 for images, they may correspond to pixel intensities, color values, or transformed coefficients; and
041 for other domains, analogous discrete representations are used.

042 Lossless compression works by exploiting regularities in the data: common patterns are assigned
043 shorter codes, while rare patterns receive longer ones. These regularities may reflect simple statis-
044 tics, such as symbol frequencies, or more complex and context-dependent structure and even se-
045 mantic information. From this perspective, any lossless compression method implicitly defines a
046 probabilistic model of the data source, with compression effectiveness depending on how well the
047 model matches the true distribution. Some algorithms make this explicit, using predictive models
048 that estimate the probability of each symbol given its context [Cleary & Witten (1984)] in order to
049 generate the code; we refer to such algorithms as *model-driven*. Others, such as Lempel–Ziv–Welch
050 (LZW), ZIP, or bzip2, achieve their gains through dictionary-building or transforms, but nonetheless
051 rely on an implicit statistical model of the domain.¹

052 In model-driven compression, the message is encoded sequentially, and for each symbol the model
053 makes a probabilistic prediction based on the context of the prior symbols so the encoding can more

¹They can even be used to create explicit predictive models [Delétang et al. (2024)].

054 efficiently allocate bits to potential outcomes. To convert the predictive model into a compression
055 algorithm, the standard technique is to pair the model with arithmetic coding [Pasco (1976); Ris-
056 sanen (1976); Guazzo (1980)]. Arithmetic coding represents an entire message as a subinterval of
057 $[0, 1]$, successively narrowing the interval according to the predicted probabilities of each symbol.
058 More probable symbols shrink the interval less and thus yield shorter average descriptions, while
059 less probable symbols shrink it more and thus require more bits. Unlike Huffman coding [Huffman
060 (1952)] (another commonly used technique), arithmetic coding adapts particularly well to changing
061 and context-dependent probabilities for each symbol. If the model closely reflects the true distribu-
062 tion of the data, arithmetic coding yields compression rates approaching the information-theoretic
063 limit. However, it is extremely sensitive to numerical precision, and small deviations can propagate
064 through the algorithm.

065 Model-driven lossless compression has a long history, arguably going back to Shannon (1948),
066 where Shannon tallies frequencies of characters in English, building first, second, and third order
067 Markov model predictions. The arithmetic coding approach for model-driven compression was
068 discussed by Cleary & Witten (1984) and further developed with a number of statistical or learned
069 predictive models across many domains. Many of these models focus on deriving the prediction
070 model from only the previously seen encoded symbols. In Schmidhuber & Heil (1996), it is clarified
071 that “offline” models are those trained on a separate files and model parameters are shared among
072 all machines responsible for encoding and decoding. In contrast “online” models use the current file
073 to update predictions. Schmidhuber & Heil (1996) use offline neural networks and get competitive
074 compression ratios. Many other works since, Knoll (2025); Cox (2016); Goyal et al. (2018); Bellard
075 (2019); Liu et al. (2019) have used LSTMs and other recurrent neural networks as predictive models.
Transformers were used as the predictive model in Bellard (2019; 2021); Mao et al. (2022).

076 This general arithmetic coding-based lossless compression technique, particularly when paired with
077 modern neural network-driven predictive models, has been shown to have significant promise in
078 numerous domains beyond text compression. These domains include lossless image compression
079 Toderici et al. (2016); Schiopu et al. (2018); Mentzer et al. (2019); Rhee et al. (2022); Chen et al.
080 (2024), compression of large numerical datasets such as time-series power data Ma et al. (2022),
081 and neural network checkpoints Kim & Belyaev (2025).

082 The incredible success of modern neural networks, particularly transformers, for natural language
083 processing has led to increased interest in using the model-driven approach to create more powerful
084 and context-adaptive codes for natural language compression. Recent work by Delétang et al. (2024)
085 shows that offline model-driven compression using modern models such as Llama 2 or Chinchilla
086 with arithmetic coding can deliver significant improvement over state-of-the-art lossless compres-
087 sion algorithms across domains including text and vision. Concurrently, LLM-driven text compres-
088 sion tools such as LLMZip [Valmeekam et al. (2023)] and llama-zip [Buzanis (2024)] were
089 introduced to take advantage of the capabilities of these advanced models.

091 1.2 LLM NON-DETERMINISM AND PREDICTION MISMATCH

092 Despite its promise, LLM-driven compression faces serious practical obstacles. For instance, the
093 LLM inference pipeline must run for each token during the encoding and decoding steps, which can
094 make the process prohibitively slow, since large language models are often computationally expen-
095 sive to execute. This also requires the model, which may contain many gigabytes of parameters,
096 to be stored, thus adding a large overhead cost in memory as well. Recent work, such as has been
097 done to address concerns about the computational performance of LLM-driven compression, such
098 as Mittu et al. (2024) on improving speeds for LLMZip.

100 Another significant challenge, which we call *prediction mismatch*, arises when compressed data is
101 transmitted between an encoder and decoder running on different machines. As noted in Witten
102 et al. (1987), arithmetic coding with adaptive probability models, “It must be possible for the de-
103 coder to produce exactly the same probability distribution in the same context”. Achieving this is
104 unexpectedly difficult with modern machine learning models due to *LLM non-determinism*.

105 Non-determinism in the setting of machine learning and scientific computing means that multiple
106 runs of the same program with identical inputs (and identical random seeds) can produce different
107 outputs [Cooper et al. (2022); Semmelrock et al. (2025)]. One source of non-determinism occurs
in GPU hardware: floating point operations which are performed in a different order may result in

108 different outcomes due to rounding. These small numerical deviations, in a full inference pipeline
109 run, can cascade into large differences in what a model predicts [Shanmugavelu et al. (2025); Chen
110 et al. (2022)]. GPU libraries, like CUDA and cuDNN, state specifically in their documentation
111 that they do not guarantee determinism or reproducibility in many circumstances, such as when
112 different versions or architectures are used [NVIDIA Corporation (2025a;b)]. The effects of non-
113 determinism in CUDA is studied in Eryilmaz et al. (2024) where they note that non-determinism is
114 likely to remain in CUDA because of the runtime benefits CUDA gains through using parallelism.
115 Non-determinism in GPUs have also been examined and explored by Morin & Willetts (2020).
116 Works such as Coakley et al. (2022) and Atil et al. (2025) examined the issue of non-determinism
117 experimentally, finding significant variability, and Schlägl et al. (2023) study its causes.

118 Applying arithmetic coding directly under these conditions is usually immediately fatal: even subtle
119 differences in the encoder and decoder probability distributions can result in an incorrectly decoded
120 token, which then cascades to the rest of the message as it changes the context of subsequent tokens.

121 If the mismatch between the encoder and decoder distributions is arbitrarily large, recovery is im-
122 possible. However, if the mismatch is known to be small, they can exploit this closeness to reach
123 exact agreement on a third probability distribution. This robustness incurs a cost in compression
124 efficiency: the encoder will generally have to send extra information to ensure agreement, and the
125 agreed probability distribution may be less accurate than the original predictions. We refer to the
126 problem of constructing a shared distribution while minimizing the cost as *probability matching*.

128 1.3 CONTRIBUTIONS

130 This work introduces the probability matching problem as a framework for addressing prediction
131 mismatch in model-driven lossless compression and proposes *PMATIC* (Probability-Matched
132 Interval Coding) to address it. PMATIC is designed to convert any predictive model into a compression
133 algorithm which is robust to bounded prediction mismatch, and to be a drop-in replacement for
134 arithmetic coding in model-driven compression. This work also shows the following results:

- 135 • *Theory*: We prove that PMATIC guarantees correct decoding under a simple and general
136 model of bounded prediction mismatch (Section 2.1), and give theoretical bounds on the
137 cost incurred to ensure this robustness.
- 138 • *Practice*: We demonstrate experimentally that LLM-driven compression using PMATIC
139 achieves compression ratios significantly better than current standard methods, while re-
140 maining robust to prediction mismatch.

142 To our knowledge, this is the first work to explicitly address LLM non-determinism and prediction
143 mismatch as fundamental obstacles to model-driven compression. In Section 5, we validate our
144 approach by applying PMATIC with Llama 3.1 as the predictive model on Wikipedia data in the
145 presence of synthetically generated prediction mismatch. PMATIC is a proof of concept that small
146 amounts of variability in LLM computations can be combated in the application of data compression.

148 2 PROBLEM STATEMENT

150 Consider the case where an encoder and decoder are using the same model (such as a spe-
151 cific LLM with the same weights) to compute next-token probabilities over an input string $x =$
152 $x(1)x(2)\dots x(n)$ whose entries $x(i)$ are taken from a finite alphabet \mathcal{A} of possible symbols. We
153 use the following notation: the i -symbol prefix of x is denoted as $x^i := x(1)\dots x(i)$; the set of all
154 finite strings drawn from the alphabet \mathcal{A} is denoted as $\mathcal{A}^* := \bigcup_{i \geq 0} \mathcal{A}^i$.

156 Typically, an LLM computes its next-token probabilities by computing a real-valued (or, rather,
157 floating-point valued) weight, called a *logit*, for each outcome and then applying the *softmax* func-
158 tion to the vector of logits²Let functions $M^{\text{Enc}}, M^{\text{Dec}} : \mathcal{A}^* \rightarrow \mathbb{R}^{\mathcal{A}}$ take a string of symbols (the
159 context) and return a logit value for each symbol in the alphabet, representing what happens when
160 the model is run for inference at the encoder and decoder ends, respectively. We denote the predic-

161 ²For simplicity we use the standard softmax with a ‘temperature’ parameter of 1.

162 tions of M^{Enc} , M^{Dec} for token i (expressed as logit vectors) as
163

$$164 \quad \mathbf{u}(i) := M^{Enc}(\mathbf{x}^{i-1}) \quad \text{and} \quad \mathbf{v}(i) := M^{Dec}(\mathbf{x}^{i-1}) \quad (1)$$

165 which respectively induce probability vectors $\mathbf{p}(i) = \text{softmax}(\mathbf{u}(i))$ and $\mathbf{q}(i) = \text{softmax}(\mathbf{v}(i))$,
166 i.e. for any $i \in [n]$ and $k \in \mathcal{A}$,
167

$$168 \quad p(i)_k = \text{softmax}(\mathbf{u}(i))_k := \frac{e^{u(i)_k}}{\sum_{j \in \mathcal{A}} e^{u(i)_j}} \quad \text{and} \quad q(i)_k = \text{softmax}(\mathbf{v}(i))_k := \frac{e^{v(i)_k}}{\sum_{j \in \mathcal{A}} e^{v(i)_j}}. \quad (2)$$

170 When the token number i is fixed, we may drop it from the notation for clarity, so that the encoder
171 and decoder return logit vectors \mathbf{u}, \mathbf{v} which induce probability distributions \mathbf{p}, \mathbf{q} respectively.
172

173 We denote the encoding and decoding algorithms (also called compressing and decompressing, re-
174 spectively) as functions whose operation depends on an LLM model (M^{Enc} and M^{Dec} respectively)
175 as well as on more traditional inputs. Specifically, the encoder takes LLM M^{Enc} and input token
176 string \mathbf{x} and returns a bitstring \mathbf{b} which is the encoded input. Then, the decoder takes \mathbf{b} and its own
177 LLM M^{Dec} and returns a decoded string $\hat{\mathbf{x}}$:

$$178 \quad \text{Enc}(M^{Enc}; \mathbf{x}) = \mathbf{b} \quad \text{and} \quad \text{Dec}(M^{Dec}; \mathbf{b}) = \hat{\mathbf{x}}. \quad (3)$$

180 Given a constraint on the difference between M^{Enc} and M^{Dec} 's outputs on any given context, we
181 say that the algorithm is *mismatch-tolerant* with respect to that constraint if, for all M^{Enc}, M^{Dec} that
182 satisfy the constraint,

$$184 \quad \text{Dec}(M^{Dec}; \text{Enc}(M^{Enc}; \mathbf{x})) = \mathbf{x} \quad \text{for all } \mathbf{x}. \quad (4)$$

185 The goal is to design algorithms which can tolerate a given amount of mismatch between the encoder
186 and decoder probability distributions while minimizing the cost in compression efficiency.
187

188 2.1 THE BOUNDED PREDICTION MISMATCH SETTING

190 Since the encoder and decoder are using the same LLM on the same inputs, it is reasonable to
191 assume that they obtain logits whose difference is bounded by some reasonably small $\varepsilon > 0$. A
192 natural choice for this is to assume that their difference has bounded L_∞ norm (i.e. elementwise):
193 $\|\mathbf{u} - \mathbf{v}\|_\infty := \max_{k \in \mathcal{A}} |u_k - v_k| \leq \varepsilon$. We first define the following a measure of difference between
194 two probability distributions:

195 **Definition 1.** *The conditional total variation distance (d_{CTV}) between two probability distributions
196 \mathbf{p}, \mathbf{q} on an alphabet \mathcal{A} is defined as the maximum total variation distance (d_{TV}) of \mathbf{p} and \mathbf{q} after
197 conditioning on some (nonempty) $S \subseteq \mathcal{A}$, i.e.*

$$198 \quad d_{CTV}(\mathbf{p}, \mathbf{q}) := \max_{\emptyset \neq S \subseteq \mathcal{A}} d_{TV}(\mathbf{p}(\cdot|S), \mathbf{q}(\cdot|S)) \quad (5)$$

200 where $\mathbf{p}(\cdot|S)$ and $\mathbf{q}(\cdot|S)$ are, respectively, \mathbf{p} and \mathbf{q} conditioned on the outcome being in S .
201

202 Note that there is no divide-by-zero issue with conditioning on any (nonempty) S since all probabili-
203 ties are induced via the softmax function and hence strictly positive. Bounded prediction mismatch
204 then bounds conditional TV distance:

205 **Proposition 1.** *If \mathbf{u}, \mathbf{v} induce probability distributions $\mathbf{p} = \text{softmax}(\mathbf{u})$ and $\mathbf{q} = \text{softmax}(\mathbf{v})$ over
206 \mathcal{A} , and $\|\mathbf{u} - \mathbf{v}\|_\infty \leq \varepsilon$, then $d_{CTV}(\mathbf{p}, \mathbf{q}) \leq \frac{\varepsilon}{2}$.*

208 *Proof.* Using the definition of TV distance, the conditional TV distance can be rewritten as

$$209 \quad d_{CTV}(\mathbf{p}, \mathbf{q}) = \max_{\substack{\emptyset \neq S \subseteq \mathcal{A} \\ S^* \subseteq S}} |p(S^*|S) - q(S^*|S)| \quad (6)$$

$$212 \quad \Rightarrow \quad \max_{\|\mathbf{u} - \mathbf{v}\|_\infty \leq \varepsilon} d_{CTV}(\mathbf{p}, \mathbf{q}) = \max_{\|\mathbf{u} - \mathbf{v}\|_\infty \leq \varepsilon} \max_{\substack{\emptyset \neq S \subseteq \mathcal{A} \\ S^* \subseteq S}} |p(S^*|S) - q(S^*|S)| \quad (7)$$

$$214 \quad = \max_{\emptyset \neq S \subseteq \mathcal{A}} \max_{\|\mathbf{u} - \mathbf{v}\|_\infty \leq \varepsilon} |p(S^*|S) - q(S^*|S)| \quad (8)$$

216 So, if $\max_{\|\mathbf{u}-\mathbf{v}\|_\infty \leq \varepsilon} |p(S^*|S) - q(S^*|S)| \leq \frac{\varepsilon}{2}$ for all $S^* \subseteq S \subseteq \mathcal{A}$, then $\max_{\|\mathbf{u}-\mathbf{v}\|_\infty \leq \varepsilon} d_{\text{CTV}}(\mathbf{p}, \mathbf{q}) \leq \frac{\varepsilon}{2}$.
217

218 In other words, the conditional TV distance between \mathbf{p}, \mathbf{q} induced by $\|\mathbf{u}-\mathbf{v}\|_\infty \leq \varepsilon$ can be bounded
219 by first fixing $S^* \subseteq S \subseteq \mathcal{A}$ and then bounding $|p(S^*|S) - q(S^*|S)|$ over all \mathbf{p}, \mathbf{q} whose logits are
220 within ε of each other in L_∞ distance. We assume WLOG that the \mathbf{u}, \mathbf{v} maximizing $|p(S^*|S) -$
221 $q(S^*|S)|$ has $q(S^*|S) > p(S^*|S)$ (otherwise S^* can be changed into $S \setminus S^*$), so the goal is to
222 maximize $q(S^*|S) - p(S^*|S)$ given the logit L_∞ bound. This is achieved by letting

$$v_k = u_k + \varepsilon \text{ for } k \in S^* \quad \text{and} \quad u_k - \varepsilon \text{ for } k \notin S^* \quad (9)$$

224 Let $p^* := p(S^*|S)$ and $q^* := q(S^*|S)$, which are both scalars in $[0, 1]$. Then, given (9),
225

$$q^* = \frac{\sum_{k \in S^*} e^{u_k + \varepsilon}}{\sum_{k \in S^*} e^{u_k + \varepsilon} + \sum_{k \in S \setminus S^*} e^{u_k - \varepsilon}} = \frac{e^\varepsilon p^*}{e^\varepsilon p^* + e^{-\varepsilon}(1 - p^*)} \quad (10)$$

$$\implies q^* - p^* \leq \max_{p^* \in [0, 1]} \left(\frac{e^\varepsilon p^*}{e^\varepsilon p^* + e^{-\varepsilon}(1 - p^*)} - p^* \right) = \tanh\left(\frac{\varepsilon}{2}\right) \leq \frac{\varepsilon}{2}. \quad (11)$$

231 Tracing this bound back to the conditional TV distance concludes the proof. \square
232

3 THE PMATIC ALGORITHM

235 The Probability Matching Interval Coding (PMATIC) algorithm addresses prediction mismatch by
236 ensuring that the encoder and decoder use a common probability distribution for each token. The first
237 step of PMATIC is to convert the input token string into a bitstring using a dictionary that associates
238 each token with a length- $\ell := \lceil \log_2(|\mathcal{A}|) \rceil$ bitstring. We will call each bit in this bitstring a *token bit*.
239 PMATIC encodes these tokens bits with arithmetic coding using next-bit conditional probabilities
240 derived from the token's encoder prediction vector. At each step, the next-bit prediction is a scalar
241 in $[0, 1]$ giving the probability that the token bit equals 1. The key idea is to divide the interval
242 $[0, 1]$ into a set of *bins* (disjoint equal-length intervals which cover $[0, 1]$). Then, instead of using
243 their exact predictions, the encoder and decoder use either the center of the bin their predictions
244 fall into or the nearest boundary between two bins; which one to use is decided by the encoder and
245 communicated to the decoder by use of auxiliary 'helper' bits, which are also sent via arithmetic
246 coding. This procedure can be viewed as quantizing the probability of each token bit.

246 For any token x_i in the message, we denote its corresponding bitstring by $\mathbf{b}_i := b_i(1) \dots b_i(\ell)$ and
247 define the following parameters and notation:
248

- 249 • $\delta > 0$, which represents the amount of prediction mismatch (per bit) which the algorithm
250 can tolerate, as measured by conditional TV distance.
- 251 • $r > 0$ is the radius of the quantization bins (so the width of a bin is $2r$); r will be chosen
252 to maximize performance given δ . We will assume that $r = 1/(2m)$ for some integer m ;
253 in practice this entails rounding r up or down slightly to the nearest such value, which will
254 still be at the correct scale relative to δ . We also always set $r > 2\delta$.
- 255 • Let $h(p) := p \log\left(\frac{1}{p}\right) + (1 - p) \log\left(\frac{1}{1-p}\right)$ be the binary entropy function (the entropy of
256 a Bernoulli random variable with probability p), and $H(\mathbf{p})$ be the more general entropy
257 function for a probability vector \mathbf{p} over a finite set.
- 258 • Let $D_{\text{KL}}(p\|q) := p \log\left(\frac{p}{q}\right) + (1 - p) \log\left(\frac{1-p}{1-q}\right)$ be the binary Kullback Liebler divergence
259 (the divergence between two Bernoulli random variables with probabilities p, q respectively).
- 260 • Let $S_{\mathbf{b}_i^{j-1}} := \{\mathbf{a} \in \{0, 1\}^\ell : \mathbf{a}^{j-1} = \mathbf{b}_i^{j-1}\}$ denote the set of length- ℓ bitstrings whose first
261 $j - 1$ bits agree with \mathbf{b}_i .

3.1 THE PMATIC ENCODER

265 Consider encoding the j th bit, $b_i(j)$, of token x_i . Let the encoder and decoder prediction vectors for
266 token i be, respectively, $\mathbf{p}(i) := \text{softmax}(\mathbf{M}^{\text{Enc}}(\mathbf{x}^{i-1}))$ and $\mathbf{q}(i) := \text{softmax}(\mathbf{M}^{\text{Dec}}(\mathbf{x}^{i-1}))$. The
267 predictions for the j th bit $b_i(j)$ for the encoder and decoder, conditional on the prior bits in \mathbf{b}_i , are
268

$$p_i(j) := \mathbb{P}_{\mathbf{p}(i)} \left[b_i(j) = 1 \mid S_{\mathbf{b}_i^{j-1}} \right] \quad \text{and} \quad q_i(j) := \mathbb{P}_{\mathbf{q}(i)} \left[b_i(j) = 1 \mid S_{\mathbf{b}_i^{j-1}} \right] \quad (12)$$

270

271

Case 1: probability not near edge
 • helper bit = 0
 • quantize with original binning



272

273

274

275

276

277

Figure 1: Examples of PMATIC helper-bit and quantization logic for two cases, one where the helper bit is 0 and one where the helper bit is 1.

278

279

280

281

These can be computed directly using $p(i)$ (or $q(i)$) by setting all values outside of $S_{b_i^{j-1}}$ to 0 and renormalizing to get the conditional probability distribution.

282

283

The interval $[0, 1]$ is then split into radius- r intervals, which we call *bins*, I_1, I_2, \dots, I_m , where $m = 1/(2r)$ (which, as assumed above, is an integer) and $I_k = [2r(k-1), 2rk]$. The center of bin I_k is therefore $c_k := 2r(k-1) + r$, and we denote the δ -*interior* of I_k (the set of points in I_k at least δ away from any point outside I_k) by

284

285

286

287

$$I_k^\delta = \begin{cases} [0, 2r - \delta] & \text{if } k = 1 \\ [2r(m-1) + \delta, 1] & \text{if } k = m \\ [2r(k-1) + \delta, 2rk - \delta] & \text{if } k \neq 1, m \end{cases} \quad (13)$$

288

289

290

291

I_1^δ, I_m^δ need special definition as they have an edge next to the edge of $[0, 1]$ instead of another bin.

292

293

294

295

Note that if $p_i(j) \in I_k^\delta$ and $|p_i(j) - q_i(j)| \leq \delta$, then $q_i(j) \in I_k$, and that if $p_i(j) \notin I_k^\delta$ for all k , then there is instead a unique integer $k \neq 1, m$ for which $|2rk - p_i(j)| < \delta$.

296

297

In addition to the token bit $b_i(j)$, PMATIC encodes (prior to the token bit) a *helper bit*

298

299

$$b'_i(j) = \begin{cases} 0 & \text{if } b_i(j) \in I_k^\delta \text{ for some } k \\ 1 & \text{otherwise} \end{cases} \quad (14)$$

300

301

This encoding is done with arithmetic coding using probabilities $p' := \delta/r$ for the helper bit and

302

303

304

$$\hat{p}_i(j) = \begin{cases} c_k = 2r(k-1) + r & \text{if } p_i(j) \in I_k^\delta \\ 2rk \text{ for the integer } k \text{ s.t. } |2rk - p_i(j)| < \delta & \text{otherwise} \end{cases} \quad (15)$$

305

306

for the token bit. The probability $\hat{p}_i(j)$ is the common probability of token bit j that both the encoder and decoder agree to use. See Figure 1 for an example.

307

The intuition for the helper bits is that when $p_i(j) \in I_k^\delta$, the encoder knows that the decoder's probability $q_i(j) \in I_k$ (the same bin), so the encoder quantizes to the bin center and tells the decoder to do the same by sending the helper bit $b'_i(j) = 0$. If $p_i(j)$ is not in the δ -interior of its bin, the encoder no longer knows that the decoder probability lies in the same bin. However, in this case both probabilities must be near the same boundary point between two bins, so the encoder quantizes to the nearest boundary point and tells the decoder to do the same by sending the helper bit $b'_i(j) = 1$. In either case, they agree on the probability to use for encoding and decoding. The probability of being in the δ -interior of a bin is $\approx \delta/r$, which is very small if $r \gg \delta$. This gives the helper bits low entropy and hence makes them highly compressible via arithmetic coding.

316

317

To summarize, given a token x_i and context \mathbf{x}^{i-1} , the PMATIC encoder does the following:

318

319

320

321

322

323

1. Computes $\mathbf{p}(i) = \text{softmax}(\mathbf{M}^{\text{Enc}}(\mathbf{x}^{i-1}))$, gets the bitstring \mathbf{b}_i corresponding to x_i , and computes the conditional next-bit probabilities $p_i(1), \dots, p_i(\ell) \in [0, 1]$.
2. Computes for each bit $b_i(j)$ the helper bit $b'_i(j)$ and quantized probability $\hat{p}_i(j)$ ((14), (15)).
3. Encodes the bitstring $b'_i(1)b_i(1) \dots b'_i(\ell)b_i(\ell)$ using arithmetic coding, where the encoding probability for each helper bit $b'_i(j)$ is $p' = \delta/r$ and the encoding probability for each token bit $b_i(j)$ is $\hat{p}_i(j)$.

324 3.2 THE PMATIC DECODER
 325

326 The PMATIC decoder takes the encoded message \mathbf{y} and decodes it sequentially in pairs of bits.
 327 Each pair consists of a helper bit and a token bit; the helper bit is decoded first using $p' = \delta/r$
 328 as the probability (since helper bits are always encoded using this probability), and determines the
 329 quantized probability to use. Analogous to the encoder next-bit prediction, let the decoder next-bit
 330 prediction for bit j of token i be denoted $q_i(j)$. Then the decoder decodes the token bit using the
 331 quantized probability:

332
$$\hat{q}_i(j) = \begin{cases} c_k \text{ for } k \text{ s.t. } q_i(j) \in I_k & \text{if } b'_i(j) = 0 \\ 2rk \text{ for } k \in \{1, \dots, m-1\} \text{ s.t. } |2rk - q_i(j)| \text{ is minimized} & \text{if } b'_i(j) = 1 \end{cases} \quad (16)$$

 333

335 After decoding all the bits, the helper bits are discarded and the token bits are converted back into
 336 a token string using the token-bitstring dictionary. PMATIC is successful when $\hat{q}_i(j)$ is the same as
 337 $\hat{p}_i(j)$ produced in the encoder step. This is discussed in greater detail in the next section.
 338

339 4 ANALYSIS
 340

341 We wish to: (i) show that PMATIC ensures correct decoding if the conditional TV distance be-
 342 tween the encoder and decoder token predictions is at most δ ; (ii) show (in expectation) theoretical
 343 performance bounds. Since we compress in bits, all logarithms are base-2 unless noted otherwise.
 344

345 4.1 CORRECTNESS
 346

347 **Theorem 1.** *If $d_{\text{CTV}}(\mathbf{p}(i), \mathbf{q}(i)) \leq \delta$, then $\hat{q}_i(j) = \hat{p}_i(j)$ for all j (i.e. the encoder and decoder will
 348 agree on the quantized probabilities for all bits corresponding to token x_i).*
 349

350 *Proof.* Consider bit j of token i ; without loss of generality we can assume that all previous bits in i
 351 and all previous tokens were decoded correctly (since, if any bits are incorrectly decoded, there must
 352 be a first one). Since $d_{\text{CTV}}(\mathbf{p}(i), \mathbf{q}(i)) \leq \delta$, we know that $|p_i(j) - q_i(j)| \leq \delta$ (since $p_i(j), q_i(j)$ are
 353 derived by conditioning $\mathbf{p}(i), \mathbf{q}(i)$ on the outcome coming from the set $S_{b_i^{j-1}}$).
 354

355 First, the decoder will decode the helper bit $b'_i(j)$ using the probability δ/r . Since δ/r is fixed and
 356 used for all helper bits, the encoder and decoder probabilities match and the helper bit is decoded
 357 correctly. Now we consider two cases: $b'_i(j) = 0$, and $b'_i(j) = 1$.

358 If $b'_i(j) = 0$, this means that computed encoder next-bit predictor $p_i(j)$ falls in the δ -interior I_k^δ of
 359 some bin; since $|p_i(j) - q_i(j)| \leq \delta$, this means $q_i(j) \in I_k$ (not necessarily the δ -interior, just the
 360 bin itself). Thus, since both the encoder and decoder quantize to the center c_k of the bin, we have
 361 $\hat{p}_i(j) = \hat{q}_i(j) = c_k$ and the token bit is encoded correctly.

362 If $b'_i(j) = 1$, then there is some $k \in \{1, \dots, m-1\}$ such that $|p_i(j) - 2rk| \leq \delta$ (note that $2rk$ here
 363 is the boundary between two bins). Then, since we set $r > 2\delta$ and bins have width $2r$:

365 $|p_i(j) - 2rk| \leq \delta \implies |q_i(j) - 2rk| \leq 2\delta \quad (17)$
 366

367 $\implies |q_i(j) - 2rk'| \geq 2r - 2\delta > 2\delta \text{ for any integer } k' \neq k \quad (18)$
 368

369 $\implies \hat{q}_i(j) = 2rk = \hat{p}_i(j). \quad (19)$

370 Thus, in either case, the encoder and decoder agree on the next-bit probability for $b_i(j)$ and the
 371 decoder will decode the bit and update the arithmetic code interval correctly. \square
 372

373 Note that, by Theorem 1 and Proposition 1, if the LLM has logits that differ by at most ε between
 374 the encoder and decoder, then compressing with PMATIC using $\delta = \varepsilon/2$ guarantees correctness.
 375

376 4.2 COMPRESSION LOSS
 377

For the compression performance analysis, we make the following simplifying assumptions:

378 • The encoder’s next-token probabilities are the true probabilities. This means that the ex-
 379 pected increase in message length for each bit $b_i(j)$ is $D_{\text{KL}}(p_i(j) \parallel \hat{p}_i(j))$ (Cover & Thomas,
 380 2006, Thm 5.4.3), and that the no-mismatch optimal expected message length per token x_i
 381 is $H(\mathbf{p}_i)$ where $H(\cdot)$ is the entropy.
 382 • Within each individual bin, the encoder next-bit probability is roughly uniformly distributed
 383 (so e.g. it’s not disproportionately likely to fall next to the bin boundary and the probability
 384 of being within δ of a bin boundary is $\approx \delta/r$).³
 385

386 We consider the *compression loss* of PMATIC over traditional (non-mismatch-tolerant) arithmetic
 387 coding, i.e. the extra message length incurred by PMATIC in order to tolerate a conditional TV
 388 distance bound of δ with a bin width of r . This loss comes from two sources:

389 1. *Helper bit encoding*: the helper bits require extra message bits to send. Since all helper bits
 390 are (approximately) Bernoulli with parameter δ/r , the expected extra encoding length per
 391 helper bit is the binary entropy $h(\delta/r) = \frac{\delta}{r} \log\left(\frac{r}{\delta}\right) + \left(\frac{r-\delta}{r}\right) \log\left(\frac{r}{r-\delta}\right)$.
 392 If $r \gg \delta$, then the first term dominates and the entropy of each helper bit is $\approx \frac{\delta}{r} \log\left(\frac{r}{\delta}\right)$.
 393 2. *Quantization loss*: the quantized probability $\hat{p}_i(j)$ is different than the true probability
 394 $p_i(j)$, incurring a quantization loss of $D_{\text{KL}}(p_i(j) \parallel \hat{p}_i(j))$.
 395 Since $r \leq \hat{p}_i(j) \leq 1-r$ (all bin centers and boundaries are in $[r, 1-r]$) and $|p_i(j) - \hat{p}_i(j)| \leq r$,
 396 the quantization loss satisfies $D_{\text{KL}}(p_i(j) \parallel \hat{p}_i(j)) \leq 2 \log(e)r$, since KL divergence is
 397 bounded above by χ^2 divergence (Polyanskiy & Wu, 2025, Ch. 7):
 398

$$D_{\text{KL}}(p_i(j) \parallel \hat{p}_i(j)) \leq \log(e) \frac{(p_i(j) - \hat{p}_i(j))^2}{\hat{p}_i(j)(1 - \hat{p}_i(j))} \leq 2 \log(e)r \quad (20)$$

402 since the numerator is $\leq r^2$ and the denominator is $\geq (1/2)r$.
 403

404 Note that these losses respond in opposite directions when the bin radius r is increased: larger bins
 405 mean lower helper bit entropy but a bigger difference between the true probability and the quantized
 406 probability. This means that setting r to balance the loss terms gives an approximate minimizer of
 407 the objective function: any other $r' \neq r$ will make one of the loss terms larger, so balancing the loss
 408 terms incurs a total loss of at most 2 times the optimal. This is achieved (approximately) with

$$2 \log(e)r = \frac{\delta}{r} \log\left(\frac{r}{\delta}\right) \implies r \approx \frac{\sqrt{\delta \log\left(\frac{1}{\delta}\right)}}{\sqrt{2 \log e}} \quad (21)$$

413 and yields a total loss on the order of $O(\sqrt{\delta \log\left(\frac{1}{\delta}\right)})$ (note that one of the loss terms is itself $O(r)$,
 414 so the total loss should be proportional to r when balancing the loss terms).
 415

416 5 EXPERIMENTS

419 We test PMATIC on text using different (quantized) LLMs as the predictive model and synthetic
 420 mismatched probabilities, and compare to standard baselines and non-mismatch-robust LLM-driven
 421 compression.

423 5.1 SETUP

425 The three models we use are LLaMA 3.1 8B (4-bit quantized), Mistral 7B v0.1 (3-bit quantized) and
 426 Qwen 2.5 Instruct 7B (3-bit quantized). Llama 3.1 8B [Grattafiori et al. (2024)] includes a tokenizer
 427 with a 128, 256-token vocabulary, whereas the Mistral and Qwen models we used respectively have
 428 a 32, 000-token vocabulary and a 151, 643-token vocabulary.

429 ³This assumption is reasonable and holds up well in practice if the bins are relatively small. If desired,
 430 PMATIC can modified so that this assumption is not necessary for the analysis, by adding a PRNG (pseudo-
 431 random number generator) to the encoder and decoder to (pseudo)randomly translate the bins by a value within
 432 $[-r, r]$. This ensures that for any $p_i(j)$, it has at most δ/r chance of being within δ of a bin boundary.

Parameter Settings	Fraction of Helper Bits Equal to 1	Helper Bit Fraction of Encoded Text
no PMATIC	0	0
$\delta = 10^{-5}, r = 0.005$	0.00051	0.04594
$\delta = 10^{-3}, r = 0.05$	0.00368	0.18947
$\delta = 10^{-2}, r = 0.125$	0.01145	0.34073

438 Figure 2: Helper bit behavior averaged across different PMATIC robustness parameter settings.
 439

440 We run our experiment on several datasets. One of these datasets is the first (nearly) 10 MB of the
 441 enwik8 benchmark Hutter (2006), consisting of a collection of Wikipedia articles from 2006 with
 442 non-ASCII characters removed. The second dataset consists of 1000 randomly selected articles from
 443 Wikipedia (pulled in September 2025) with non-ASCII characters removed. The other datasets
 444 include two additional English texts, *Hamlet* by Shakespeare and *Emma* by Austen. We also use
 445 *Candide* by Voltaire in French, and *Dream of the Red Chamber* by Cao Xuewin in Chinese. For
 446 each dataset, except randomly selected Wikipedia articles, we split all our files into smaller files of
 447 size ≈ 5 KB and compress each file separately.

448 We run our algorithm with three choices of r, δ . One setting uses $\delta = 0.001$ and $r = 0.05$. Given
 449 $\delta = 0.001$, the approximate minimizer r given in (21) would be $r \approx 0.047$; we choose $r = 0.05$
 450 since it is close and divides $[0, 1]$ into intervals evenly. The small mismatch setting uses $\delta = 0.00001$
 451 and $r = 0.005$, with r chosen again to be on the right scale and to divide the $[0, 1]$ evenly. The large
 452 mismatch setting uses $\delta = 0.01$ and $r = 0.125$, and is chosen similarly.⁴

453 To speed up the algorithm, we use a rolling context window of maximum size 512 which resets
 454 every 256 tokens via truncation: each time the context length reaches 512, we drop the oldest 256
 455 tokens. Our program ran on a high-performance computing system with Xeon CPU nodes and Volta
 456 GPUs.

457 The first step of our processing is to tokenize each file. Since PMATIC assigns each token in the
 458 alphabet a unique fixed-length bitstring, we assign a random ℓ -bit representation (where ℓ depends
 459 on the model used⁵) for each token and convert the file to a bitstring. The same bitstring dictionary
 460 is used across all files in each setting.

461 The maximum logit mismatch is selected in each setting to be $\varepsilon = 2\delta$, to ensure the conditional
 462 TV distance is always at most δ (as per Proposition 1). The encoding of the text is done with the
 463 probabilities given by the model. We then create a synthetic mismatched probability distribution for
 464 the decoder by adding IID uniform noise from $[-\varepsilon, \varepsilon]$ to each logit of the encoder’s distribution.

465 Encoding and decoding the helper and token bits generated by PMATIC is done with arithmetic
 466 coding, using the implementation from Buzanis (2024).

468 For comparison, we include several standard compression algorithms. Among these, cmix is a
 469 compressor known for achieving the best compression ratios before LLM-driven compression. For
 470 other standard compression algorithms, we chose the compression level that optimizes for smallest
 471 file size.

473 **5.2 RESULTS**

475 PMATIC successfully decoded all files, validating our theoretical correctness result, and its per-
 476 formance validates the theoretical performance analysis. Our results show that PMATIC provides
 477 robustness to numerical deviations without significant loss over the extremely good rates of LLM-
 478 based compression on text. PMATIC increases the number of bits per token by ≈ 0.2 to tolerate a
 479 0.00002 mismatch per logit, by ≈ 2 to tolerate a 0.002 mismatch per logit and by ≈ 5 to tolerate
 480 a 0.02 mismatch per logit. Even in the setting combating the most mismatch, compression with
 481 PMATIC still achieves significantly better compression rates than the baselines used.

484 ⁴Since we chose r only through a rough approximation of the optimization process, it may be possible to
 485 improve performance by further refining the value of r .

486 ⁵For LLaMA 3.1, each token requires a length-17 bitstring representation since $\lceil \log(128, 256) \rceil = 17$.

		Enwik8	Randomly selected Wikipedia articles	Hamlet	Emma	Candide French	Dream of the Red Chamber Chinese
LLM-based Compression (with and without PMATIC)							
Meta	no PMATIC	0.0780	0.0700	0.0878	0.0606	0.1024	–
	$\delta = 10^{-5}, r = 0.005$	0.0847	0.0878	0.0952	0.0660	0.1102	–
LLaMA 3.1	$\delta = 10^{-3}, r = 0.05$	0.1353	0.1330	0.1514	0.1099	0.1683	–
	$\delta = 10^{-2}, r = 0.125$	0.2492	0.2085	0.2772	0.2113	0.2971	–
Mistral 7B	no PMATIC	0.0867	0.0737	0.1501	0.1066	–	–
	$\delta = 10^{-5}, r = 0.005$	0.0940	0.0794	0.1587	0.1134	–	–
	$\delta = 10^{-3}, r = 0.05$	0.1481	0.1198	0.2167	0.1595	–	–
	$\delta = 10^{-2}, r = 0.125$	0.2699	0.2106	0.3447	0.2610	–	–
Qwen2.5 7B	no PMATIC	0.0881	0.0824	0.1102	0.1183	0.1150	0.1268
	$\delta = 10^{-5}, r = 0.005$	0.0951	0.0880	0.1177	0.1253	0.1231	0.1345
Instruct	$\delta = 10^{-3}, r = 0.05$	0.1501	0.1315	0.1755	0.1738	0.1831	0.1879
	$\delta = 10^{-2}, r = 0.125$	0.2751	0.2297	0.3067	0.2825	0.3171	0.3073
Standard Baselines							
cmix		0.3558	0.3644	0.3865	0.3797	0.3709	0.3824
brotli	level 11	0.3524	0.3546	0.4361	0.3918	0.4442	0.4733
bzip2	level 9	0.4537	0.4605	0.4636	0.4539	0.4494	0.4727
xz	level 9	0.4647	0.4904	0.5111	0.4973	0.4866	0.5192
gzip	level 9	0.4601	0.4759	0.5007	0.4852	0.4768	0.5305
zstd	level 22	0.4676	0.4773	0.5034	0.4882	0.4851	0.5544

Figure 3: Compression ratio across different models, PMATIC parameters, and datasets; compression ratios are given by $\frac{\text{compressed file size}}{\text{uncompressed file size}}$. PMATIC overhead (cost of gaining mismatch robustness through PMATIC) for each parameter setting can be computed by subtracting the corresponding ‘no PMATIC’ compression ratio from the PMATIC compression ratio.

6 FUTURE WORK

While PMATIC has good theoretical and experimental performance in enabling model-driven compression to tolerate bounded prediction mismatch, there remain significant challenges. While PMATIC was validated using synthetic prediction mismatch, it remains to be validated on datasets that include real-world LLM prediction mismatch. A related problem is to extend PMATIC (or design another mismatch-robust coding technique) to allow for stochastically-bounded mismatch rather than mismatch with a hard upper bound for all logits. For practical usage, the tradeoff between prediction model size, compression efficiency, and computational performance should be characterized so that a model exhibiting a good balance of these characteristics can be chosen.

In addition, the fundamental limits of model-driven compression under prediction mismatch (that is, how much additional message length is mathematically required to correct a given amount of potential mismatch) remain unknown, and theoretical research into the mathematical and information-theoretic properties of the problem will be needed to address these fundamental limits.

Finally, LLM (and large neural network) non-determinism remains a significant challenge in several contexts outside of model-driven compression, such as ensuring reproducibility of experimental results in machine learning. It may be interesting to explore whether PMATIC, or similar approaches, might offer certain tools to address LLM non-determinism in these contexts.

540 REFERENCES
541

542 Berk Atil, Sarp Aykent, Alexa Chittams, Lisheng Fu, Rebecca J. Passonneau, Evan Radcliffe,
543 Guru Rajan Rajagopal, Adam Sloan, Tomasz Tadrej, Ferhan Ture, Zhe Wu, Lixinyu Xu,
544 and Breck Baldwin. Non-determinism of "deterministic" llm settings, 2025. URL <https://arxiv.org/abs/2408.04667>.
545

546 Fabrice Bellard. Lossless data compression with neural networks. URL: <https://bellard.org/nncp/nncp.pdf>, 2019.
547

549 Fabrice Bellard. Nncp v2: Lossless data compression with transformer. *Preprint at Fabrice Bellard*
550 https://bellard.org/nncp/nncp_v2.pdf, 2021.
551

552 Alexander Buzanis. Llama-zip: An llm-powered lossless compression tool. <https://github.com/AlexBuz/llama-zip>, 2024. Commit on main branch; accessed 2025-05-19.
553

554 Boyuan Chen, Mingzhi Wen, Yong Shi, Dayi Lin, Gopi Krishnan Rajbahadur, and Zhen Ming (Jack)
555 Jiang. Towards training reproducible deep learning models. In *Proceedings of the 44th Interna-*
556 *tional Conference on Software Engineering*, ICSE '22, pp. 2202–2214. ACM, May 2022. doi:
557 [10.1145/3510003.3510163](https://doi.org/10.1145/3510003.3510163). URL [http://dx.doi.org/10.1145/3510003.3510163](https://doi.org/10.1145/3510003.3510163).
558

559 Kecheng Chen, Pingping Zhang, Hui Liu, Jie Liu, Yibing Liu, Jiaxin Huang, Shiqi Wang, Hong Yan,
560 and Haoliang Li. Large language models for lossless image compression: Next-pixel prediction
561 in language space is all you need. *arXiv preprint arXiv:2411.12448*, 2024.
562

563 J. Cleary and I. Witten. Data compression using adaptive coding and partial string matching. *IEEE*
564 *Transactions on Communications*, 32(4):396–402, 1984. doi: [10.1109/TCOM.1984.1096090](https://doi.org/10.1109/TCOM.1984.1096090).
565

566 Kevin Coakley, Christine R. Kirkpatrick, and Odd Erik Gundersen. Examining the effect of imple-
567 mentation factors on deep learning reproducibility. In *2022 IEEE 18th International Conference*
568 *on e-Science (e-Science)*, pp. 397–398. IEEE, October 2022. doi: [10.1109/escience55777.2022.00056](https://doi.org/10.1109/escience55777.2022.00056). URL [http://dx.doi.org/10.1109/eScience55777.2022.00056](https://doi.org/10.1109/eScience55777.2022.00056).
569

570 A. Feder Cooper, Jonathan Frankle, and Christopher De Sa. Non-determinism and the lawlessness
571 of machine learning code. In *Proceedings of the 2022 Symposium on Computer Science and Law*,
572 CSLAW '22, pp. 1–8. ACM, November 2022. doi: [10.1145/3511265.3550446](https://doi.org/10.1145/3511265.3550446). URL [http://dx.doi.org/10.1145/3511265.3550446](https://doi.org/10.1145/3511265.3550446).
573

574 T.M. Cover and J.A. Thomas. *Elements of Information Theory (Wiley Series in Telecommunications*
575 *and Signal Processing)*. Wiley-Interscience, USA, 2006. ISBN 0471241954.
576

577 David Cox. Syntactically informed text compression with recurrent neural networks. *arXiv preprint*
578 *arXiv:1608.02893*, 2016.
579

580 Grégoire Delétang, Anian Ruoss, Paul-Ambroise Duquenne, Elliot Catt, Tim Genewein, Christo-
581 pher Mattern, Jordi Grau-Moya, Li Kevin Wenliang, Matthew Aitchison, Laurent Orseau, Marcus
582 Hutter, and Joel Veness. Language modeling is compression, 2024. URL <https://arxiv.org/abs/2309.10668>.
583

584 Bahadir Eryilmaz, Osman Alperen Koras, Jorg Schlotterer, and Christin Seifert. Investigating
585 the Impact of Randomness on Reproducibility in Computer Vision: A Study on Applications
586 in Civil Engineering and Medicine . In *2024 IEEE 6th International Conference on Cog-*
587 *nitive Machine Intelligence (CogMI)*, pp. 265–274, Los Alamitos, CA, USA, October 2024.
588 IEEE Computer Society. doi: [10.1109/CogMI62246.2024.00042](https://doi.org/10.1109/CogMI62246.2024.00042). URL <https://doi.org/10.1109/CogMI62246.2024.00042>.
589

590 Mohit Goyal, Kedar Tatwawadi, Shubham Chandak, and Idoia Ochoa. Deepzip: Lossless data
591 compression using recurrent neural networks. *CoRR*, abs/1811.08162, 2018. URL [http://arxiv.org/abs/1811.08162](https://arxiv.org/abs/1811.08162).
592

593 Aaron Grattafiori, Abhimanyu Dubey, Abhinav Jauhri, et al. The llama 3 herd of models, 2024.
URL <https://arxiv.org/abs/2407.21783>.
594

594 M. Guazzo. A general minimum-redundancy source-coding algorithm. *IEEE Transactions on In-*
595 *formation Theory*, 26(1):15–25, 1980. doi: 10.1109/TIT.1980.1056143.
596

597 David A. Huffman. A method for the construction of minimum-redundancy codes. *Proceedings of*
598 *the IRE*, 40(9):1098–1101, 1952. doi: 10.1109/JRPROC.1952.273898.
599

600 Marcus Hutter. The hutter prize for lossless compression of human knowledge. [http://prize.](http://prize.hutter1.net/)
601 hutter1.net/, 2006. Accessed: 2025-09-11.

602 Yury Kim and Evgeny Belyaev. An efficient compression of deep neural network checkpoints based
603 on prediction and context modeling, 2025. URL <https://arxiv.org/abs/2506.12000>.
604

605 Byron Knoll. cmix: A data compression program. [https://www.byronknoll.com/cmix.](https://www.byronknoll.com/cmix.html)
606 html, 2025. Accessed: 2025-09-23.
607

608 Qian Liu, Yiling Xu, and Zhu Li. Decmac: A deep context model for high efficiency arithmetic
609 coding. In *2019 International Conference on Artificial Intelligence in Information and Commu-*
610 *nication (ICAIIIC)*, pp. 438–443. IEEE, 2019.

611 Zhoujun Ma, Hong Zhu, Zhuohao He, Yue Lu, and Fuyuan Song. Deep lossless compression algo-
612 rithm based on arithmetic coding for power data. *Sensors*, 22(14), 2022. ISSN 1424-8220. doi:
613 10.3390/s22145331. URL <https://www.mdpi.com/1424-8220/22/14/5331>.
614

615 Yu Mao, Yufei Cui, Tei-Wei Kuo, and Chun Jason Xue. Trace: A fast transformer-based general-
616 purpose lossless compressor. In *Proceedings of the ACM Web Conference 2022*, pp. 1829–1838,
617 2022.

618 Fabian Mentzer, Eirikur Agustsson, Michael Tschannen, Radu Timofte, and Luc Van Gool. Practical
619 full resolution learned lossless image compression. In *Proceedings of the IEEE/CVF conference*
620 *on computer vision and pattern recognition*, pp. 10629–10638, 2019.

621 Fazal Mittu, Yihuan Bu, Akshat Gupta, Ashok Devireddy, Alp Eren Ozdarendeli, Anant Singh,
622 and Gopala Anumanchipalli. Finezip: Pushing the limits of large language models for practical
623 lossless text compression. *arXiv preprint arXiv:2409.17141*, 2024.

624

625 Miguel Morin and Matthew Willetts. Non-determinism in tensorflow resnets, 2020. URL <https://arxiv.org/abs/2001.11396>.

626

627 NVIDIA Corporation. *NVIDIA cuBLAS Library Documentation*, 2025a. URL <https://docs.nvidia.com/cuda/cublas/>. Version: CUDA cuBLAS.

628

629 NVIDIA Corporation. *NVIDIA cuDNN Backend API: Odds and Ends (Determinism and Re-*
630 *producibility)*, 2025b. URL <https://docs.nvidia.com/deeplearning/cudnn/backend/latest/developer/misc.html>. cuDNN Developer Documentation.

631

632 Richard Clark Pasco. *Source coding algorithms for fast data compression*. PhD thesis, Stanford
633 University CA, 1976.

634

635 Yury Polyanskiy and Yihong Wu. *Information Theory: From Coding to Learning*. Cambridge
636 University Press, 2025.

637

638 Hochang Rhee, Yeong Il Jang, Seyun Kim, and Nam Ik Cho. Lc-fdnet: Learned lossless image
639 compression with frequency decomposition network. In *Proceedings of the IEEE/CVF conference*
640 *on computer vision and pattern recognition*, pp. 6033–6042, 2022.

641

642 Jorma J Rissanen. Generalized kraft inequality and arithmetic coding. *IBM Journal of research and*
643 *development*, 20(3):198–203, 1976.

644

645 Ionut Schiopu, Yu Liu, and Adrian Munteanu. Cnn-based prediction for lossless coding of photo-
646 graphic images. In *2018 Picture Coding Symposium (PCS)*, pp. 16–20. IEEE, 2018.

647

648 Alex Schlögl, Nora Hofer, and Rainer Böhme. Causes and effects of unanticipated nu-
649 matical deviations in neural network inference frameworks. In A. Oh, T. Naumann,
650 A. Globerson, K. Saenko, M. Hardt, and S. Levine (eds.), *Advances in Neural In-*
651 *formation Processing Systems*, volume 36, pp. 56095–56107. Curran Associates, Inc.,
652 2023. URL https://proceedings.neurips.cc/paper_files/paper/2023/file/af076c3bdbf935b81d808e37c5ede463-Paper-Conference.pdf.

653

654 J. Schmidhuber and S. Heil. Sequential neural text compression. *IEEE Transactions on Neural*
655 *Networks*, 7(1):142–146, 1996. doi: 10.1109/72.478398.

656

657 Harald Semmelrock, Tony Ross-Hellauer, Simone Kopeinik, Dieter Theiler, Armin Haberl, Stefan
658 Thalmann, and Dominik Kowald. Reproducibility in machine learning-based research: Overview,
659 barriers and drivers, 2025. URL <https://arxiv.org/abs/2406.14325>.

660

661 Sanjiv Shanmugavelu, Mathieu Taillefumier, Christopher Culver, Oscar Hernandez, Mark Coletti,
662 and Ada Sedova. Impacts of floating-point non-associativity on reproducibility for hpc and deep
663 learning applications. In *Proceedings of the SC '24 Workshops of the International Conference on*
664 *High Performance Computing, Network, Storage, and Analysis*, SC-W '24, pp. 170–179. IEEE
665 Press, 2025. ISBN 9798350355543. doi: 10.1109/SCW63240.2024.00028. URL <https://doi.org/10.1109/SCW63240.2024.00028>.

666

667 C. E. Shannon. A mathematical theory of communication. *The Bell System Technical Journal*, 27
668 (3):379–423, 1948. doi: 10.1002/j.1538-7305.1948.tb01338.x.

669

670 George Toderici, Damien Vincent, Nick Johnston, Sung Jin Hwang, David Minnen, Joel Shor, and
671 Michele Covell. Full resolution image compression with recurrent neural networks. *CoRR*,
672 abs/1608.05148, 2016. URL <http://arxiv.org/abs/1608.05148>.

673

674 Chandra Shekhara Kaushik Valmeekam, Krishna Narayanan, Dileep Kalathil, Jean-Francois Cham-
675 berland, and Srinivas Shakkottai. Llmzip: Lossless text compression using large language models,
676 2023. URL <https://arxiv.org/abs/2306.04050>.

677

678 Ian H. Witten, Radford M. Neal, and John G. Cleary. Arithmetic coding for data compres-
679 sion. *Commun. ACM*, 30:520–540, 1987. URL <https://api.semanticscholar.org/CorpusID:3343393>.

680

681

682

683

684

685

686

687

688

689

690

691

692

693

694

695

696

697

698

699

700

701

702 A APPENDIX

704 A.1 PMATIC FULL TOKEN EXAMPLE

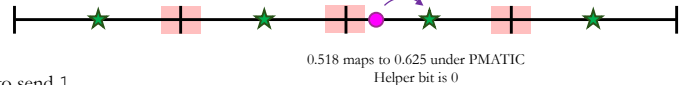
706 Illustrated here is an example of PMATIC encoding when there are 8 total tokens (each token can
707 be described by a 3-bit bitstring). PMATIC has parameter settings of $\delta = 0.01$ and $r = 0.125$ (so
708 there are four quantization bins in total).

710 Token	711 Bitstring	712 Prob
A	010	0.097
B	000	0.249
C	101	0.206
D	111	0.047
E	010	0.045
F	100	0.200
G	011	0.127
H	110	0.029

713 **PMATIC processing to send token “F” (bitstring representation 100):**

714 Bit 1: Probability bit 1 is 0

$$= 0.097 + 0.249 + 0.045 + 0.127 = 0.518$$

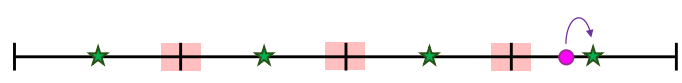


715 Need to send 1

716 Helper bit is 0

717 Bit 2: Probability bit 2 is 0 conditioned on the previous bit is 1

$$= \frac{0.206 + 0.200}{0.206 + 0.047 + 0.200 + 0.029} = 0.842 \dots$$

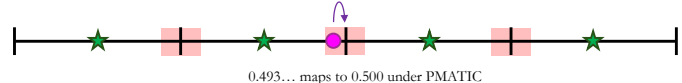


718 Need to send 0

719 Helper bit is 0

720 Bit 3: Probability bit 3 is 0 conditioned on the previous bits are 10

$$= \frac{0.200}{0.206 + 0.200} = 0.493 \dots$$



721 Need to send 0

722 Helper bit is 1

723 **Information encoded by arithmetic coder to send token f:**

724 Helper bits (where 1 occurs probability $\delta / r = 0.08$)

- 725 • 0 0 1

726 Token bits

- 727 • 1 (where 0 occurs probability 0.625)
- 728 • 0 (where 0 occurs probability 0.875)
- 729 • 0 (where 0 occurs probability 0.500)

730
731 Figure 4: Illustration of PMATIC encoding for token ‘F’. The table in the figure shows the corre-
732 sponding bitstring and model-computed probability for each token (the model-computed probability
733 depends on context).

734 A.2 LLM USAGE

735 We used LLMs (specifically GPT-5) as an assistant for the background literature search, writing, and
736 coding. This entailed asking the LLM to: search for and summarize related papers; write sample
737 paragraphs, which we could then use as a guideline for our own writing or take phrases from; and
738 explain any terms we came across which we were unsure of.

739 For the code for our experiments, we consulted LLMs in several different ways. A major design
740 choice to credit to LLMs is the idea of using a rolling context window of some maximum size when
741 getting the next token probabilities, which it suggested when asked about reducing runtime. We also
742 asked LLMs to write various small parts of the code which are standard operations, for instance, a
743 script to aggregate statistics for the experiments to be printed on the screen, a function that changes
744 byte arrays to bitstrings, some helper functions to setup arithmetic coding when running without
745 PMATIC, and even a one line function to compute entropy. LLMs were also consulted for help
746 on syntax or determining which functions to call in many places, for Linux command help and for
747 debugging. In the earlier iterations of our code, we used LLM generated code to setup the Llama

756 model, but later many of those critical parts were replaced. The key components of the PMATIC
757 algorithm were typed without the use of LLMs.
758
759
760
761
762
763
764
765
766
767
768
769
770
771
772
773
774
775
776
777
778
779
780
781
782
783
784
785
786
787
788
789
790
791
792
793
794
795
796
797
798
799
800
801
802
803
804
805
806
807
808
809